

The Effects of TiO₂ Nanoparticles on Tumor Cell Colonies: Fractal Dimension and Morphological Properties

T. Sungkaworn, W. Triampo, P. Nalakarn, D. Triampo, I. M. Tang, Y. Lenbury, and P. Picha

PACS numbers: 85.15.Aa, 87.17. Aa

Abstract—Semiconductor nanomaterials like TiO₂ nanoparticles (TiO₂-NPs) approximately less than 100 nm in diameter have become a new generation of advanced materials due to their novel and interesting optical, dielectric, and photo-catalytic properties. With the increasing use of NPs in commerce, to date few studies have investigated the toxicological and environmental effects of NPs. Motivated by the importance of TiO₂-NPs that may contribute to the cancer research field especially from the treatment prospective together with the fractal analysis technique, we have investigated the effect of TiO₂-NPs on colony morphology in the dark condition using fractal dimension as a key morphological characterization parameter. The aim of this work is mainly to investigate the cytotoxic effects of TiO₂-NPs in the dark on the growth of human cervical carcinoma (HeLa) cell colonies from morphological aspect. The *in vitro* studies were carried out together with the image processing technique and fractal analysis. It was found that, these colonies were abnormal in shape and size. Moreover, the size of the control colonies appeared to be larger than those of the treated group. The mean Df \pm SEM of the colonies in untreated cultures was 1.085 ± 0.019 , N= 25, while that of the cultures treated with TiO₂-NPs was 1.287 ± 0.045 . It was found that the circularity of the control group (0.401 ± 0.071) is higher than that of the treated group (0.103 ± 0.042). The same tendency was found in the diameter parameters which are 1161.30 ± 219.56 μ m and 852.28 ± 206.50 μ m for the control and treated group respectively. Possible explanation of the results was discussed, though more works need to be done in terms of the for mechanism aspects. Finally, our results indicate that fractal dimension can serve as a useful feature, by itself or in conjunction with other shape features, in the classification of cancer colonies.

Titawat Sungkaworn is with the Department of Biology and 6R&D Group of Biological and Environmental physics (BIOPHYSICS), Faculty of Science, Mahidol University, Bangkok 10400, Thailand.

Wannapong Triampo is with the Department of Physics and R&D Group of Biological and Environmental Physics (BIOPHYSICS), Department of Physics, Faculty of Science, and Center for Vectors and Vector-Borne Diseases, Mahidol University, Bangkok 10400, Thailand (e-mail: wtriampo@yahoo.com).

Pornkamol Nalakarn is with the 5Department of Physics, Faculty of Science & Technology, Thammasat University, and R&D Group of Biological and Environmental Physics (BIOPHYSICS), Faculty of Science, Mahidol University, Bangkok 10400, Thailand.

Daraporn Triampo is with the Department of Chemistry and R&D Group of Biological and Environmental Physics (BIOPHYSICS), Faculty of Science, Mahidol University, Bangkok 10400, Thailand.

I. Ming Tang is with the Department of Physics, Faculty of Science, Mahidol University, Bangkok 10400, Thailand.

Yongwimon Lenbury is with the Department of Mathematics, Faculty of Science, Mahidol University, Bangkok 10400, Thailand.

Pontipa Picha is with the National Cancer Institute of Thailand, Bangkok 10400, Thailand.

Keywords—Tumor growth, Cell colonies, TiO₂, Nanoparticles, Fractal, Morphology, Aggregation.

I. INTRODUCTION

SEMICONDUCTOR, nanomaterials like TiO₂ nanoparticles (TiO₂-NPs), approximately less than 100 nm in diameter, have become a new generation of advanced materials due to their novel and interesting optical, dielectric, and photo-catalytic properties from size quantization [1]. Therefore, many efforts have been devoted to produce TiO₂-NPs with controlled size, shape, and porosity for use in thin films, ceramics, composites, and catalysts. These nanometer-sized effects are caused by the large surface-to-volume ratio, resulting in more atoms along the grained boundaries than in the bulk material. It is known that the more the particles decrease in size the more attractive interactions between the particles become dominant. These attractive forces lead them to aggregate or agglomerate when the particles collide resulting in nanoparticle aggregates (NPAs) (see Fig. 1). Since the desired product properties might vary with particle size as well as the degree of aggregation or the aggregate structure, control of the particle size distribution and the aggregate structure is a key criterion to product quality. It has been accepted that NPs can exist in two states within a liquid: stable, i.e. particles separate, non-adhering and dispersed, and aggregated or flocculated, i.e. adherent and randomly clumped [2]. This clumping can occur due to van der Waals attractive forces or may be caused by magnetic or other attractions imposed by externally imposed fields. To calculate the particle-particle interaction, the DLVO theory can be employed [3]. Hence, it is very important to realize that the NPs being used in experiments, especially in suspension or colloid form have the properties (e.g., size distribution) which are different from those specified by manufactures. Moreover, in experimental processes such as sonicator, autoclave, pH and so on, may change the state or properties of the particles. Therefore, using NPs in experiments must be done with care.

With the increasing use of NPs in commerce, to date few studies have investigated the toxicological and environmental effects of NPs. Exposure to nanoparticle substances can be an important risk factor for human health. The sub-micron size of NPs offers a number of distinct advantages over

microparticles (MPs). NPs have in general relatively higher intracellular uptake rate compared to MPs. This was demonstrated in studies in which 100 nm size NPs showed 2.5 fold greater uptake compared to 1 μ m and 6 fold higher uptake compared to 10 μ m NPs in Caco-2 cell line [4]. Similar results were obtained when these formulations of NPs and MPs were tested in a rat in situ intestinal loop model. The efficiency of uptake of 100 nm sized particles was 15–250 fold greater than larger sized (1 and 10 μ m) MPs [5]. In the above rat study, it was found that NPs were able to penetrate throughout the submucosal layers while the larger size MPs were predominantly localized in the epithelial lining.

TiO₂ or titania could be used as an alternative or a complement to conventional biocidal activity technologies via photocatalysis. Photocatalytic events that occur after UVA/UVB with wavelength of less than 385nm (365 < wavelength < 385) illumination of TiO₂ (band-gap energy of anatase, 3.2 eV; for rutile, 3.0 eV) and subsequent formation of electron/hole pairs are many and very complex. Following electron/hole separation, the two charge carriers migrate to the surface through diffusion and drift, in competition with a multitude of trapping and recombination events in the lattice bulk. At the surface, these carriers are poised to initiate redox chemistry with suitable pre-adsorbed acceptor and donor molecules in competition with recombination events to yield radiative and nonradiative emissions, and/or trapping of the charge carriers into shallow traps at lattice sites (e.g., anion vacancies, Ti⁴⁺, and others). Thus, on absorption of UV light, titania particles yield superoxide radical anions and hydroxyl radicals that can initiate oxidations [6]. Photocatalytic biological inactivation has been explained by the attack of Oxygen-derived molecular species or reactive oxygen species (ROS), especially radicals photogenerated at the surface of the TiO₂ catalyst like O₂^{•-}, HO₂[•] and OH[•]. However, the mechanism of cell death or damage has not been understood yet [7].

Oxygen-derived molecular species or reactive oxygen species (ROS), such as superoxide (O₂^{•-}) and hydrogen peroxide(H₂O₂), are produced in cells as a result of aerobic metabolism. Excess generation of these species can result in damage to macromolecules such as DNA and lipids [7].

Many studies using TiO₂ photodecomposition of pollutants with the aim of developing methods to purify water and air have been carried out [8],[9],[10],[11]. For the bactericidal activity, several results have been reported using TiO₂ powder [12],[13],[14],[15],[16], and, TiO₂-coated materials for this purpose [17]. However, few studies have investigated the impacts of TiO₂ in cancer science or the field of oncology [18]. However, the actual factors that control the photocatalytic activity of specific TiO₂ particles are still unknown. Moreover, the detailed studies of the effects of TiO₂ on biological systems in dark condition were very rare. This is one of the reasons that motivate us to perform this study.

Cancer has been a leading cause of human death in the world. Not too much is known about the biological mechanisms leading to the establishment of or the growth of

malignant tumors. Many attempts have been made in recent decades to describe the basic biological mechanisms of tumor growth. Benign masses generally have smooth, circumscribed, and well-defined contours, whereas malignant tumors commonly have rough, spiculated, and ill-defined contours. Based upon this observation, shape or morphological factors such as fractal dimension (Df) have been considered.

Fractal patterns arise “spontaneously” in natural processes as a result of many microscopic interactions, and the fractal dimension is a precise measure of the morphology of a complex pattern [19],[20]. Fractal geometry is a way of quantifying natural objects with a complex geometrical structure that are difficult to quantify by regular Euclidean geometrical methods. In classical Euclidean geometry, objects have integer dimensions. For example, a line is a one-dimensional object, a plane a two-dimensional object, and a volume a three-dimensional object, with dimensions of 1, 2 & 3 respectively. In this way, Euclidean geometry is suited for quantifying objects that are ideal, man-made, or regular. One of the most important features of fractal objects is that they are self-similar; i.e., there is a repetition of patterns in the object at many different scales. In nature there is a wide range of self-organized spatial structures in multiple hierarchical levels. Surface morphology or roughness can be quantified by the value of fractal dimension, a numerical parameter having emerged from the fractal theory. This theory provides a new way to characterize irregular structure. Fractal dimension (Df) measures the space filling capacity of an object. In a fractal system, the fractal dimension of the system is less than the dimension d of the space in which the system is embedded. In recent years, the geometry of fractals has been applied to a surprising set of phenomena including electrochemical deposition [21], the architecture of physiological systems such as the bronchial tree [22], taxonomy [23], and clusters of stars [20]. Study of the fractal structure has intensified in a number of biological structures and their growth patterns in past recent years[24],[25],[26],[27],[28],[29],[30],[31],[32],[33],[34],[35]

Motivated by the importance of TiO₂-NPs that may contribute to the cancer research field especially from the treatment prospective combined with the fractal analysis technique that has proved to be useful in many fields including life science, the aim of the present study was to investigate the effect of NPs on colony morphology using fractal dimension as a key morphological characterization parameter. To the best of our knowledge, this is the first published literature on this problem.

II. MATERIALS AND METHODS

A. TiO₂ Nanoparticles

TiO₂ (P25, Sigma-Aldrich) with a surface area of 10-20 m²/g and primary particles whose size of 60-100 nm were used in experiments. The particles were suspended in sterile water and sonicated for 15 min before experiment. All processes were performed in darkness.

B. Cell Culture

Human cervical carcinoma cells (HeLa), obtained from National Cancer Institute, Thailand were cultured in EMEM (BioWhittaker), pH 7.2, supplemented with 10% NCS (BioWhittaker), penicillin (100 U/ml) and streptomycin (100 µg/ml) at 37°C in a humidified atmosphere of 5% CO₂.

C. Colony-Forming Assay

HeLa cells in exponential phase were trypsinised and counted by a Hemocytometer. Then, cell suspension was diluted and plated in 6 well cultured clusters (Corning) with TiO₂. Sterile water was used as control. After culturing for 10 days, the colonies were stained with 10% Giemsa solution (Merk) and then photographed under inverted microscope with a coupled digital camera. If the cell colony is successfully grow, i.e., colony forming efficiency more than 80% control condition, (the size and shape of the cells are as shown in Fig. 2.), the morphology will be observed by inverted phase-contrast microscopy and analyzed.

D. Image Processing and Fractal Dimension Calculation

Image processing and fractal dimension (Df) calculation via the box-counting method (BCM) were performed by using ImageJ shareware program from NIH Laboratory (<http://rsb.info.nih.gov/ij/>). BCM, is one of the most widely used [36],[37],[38] due to the relative ease of mathematical calculations and computations involved. It basically consists of drawing successively larger boxes and counting the number of boxes that touch particles (any color different from background color). The slope of the log-log plot of the number of boxes vs. their respective size is the fractal dimension.

For image processing (see Fig. 3), firstly, the acquired images were converted from RGB to 8-bit format images. Via automatic default threshold function, we can get black and white images with binary bit, namely 0 (totally black) to 255 (completely white). We then “clean up” the image and leaving only the boundary outline with the image of size 2592 x 1944 (this is one of the control parameters). Finally, we can evaluate the fractal dimension with the output sample as seen in Fig. 4.

To have confidence in our tool as to whether the software is installed or set up properly, the BCM has then been validated with a known fractal dimension structure. For the triangular Sierpinski gasket 12, the initiator is a filled triangle shown as Fig. 5. The fractal curve obtained in the limit of an infinite number of generations has the fractal dimension $D = \ln 3 / \ln 2 = 1.585$. The dimension obtained by the box size method using ImageJ software is equal to 1.579, which is accurate up to 0.379%. In addition, we also tested the software on the Koch Curve 6, and it was found that, with the theoretical value = 1.262, a our software yielded 1.267, so that the error is within 1.041% (see Fig. 5).

III. RESULTS AND DISCUSSION

In this section we present some experimental results of TiO₂-NPs-induced changes in cell colonies. Tumor cell colonies were grown in vitro, so that the nutrient concentration was uniform along the colonies. A control set of colonies was grown without TiO₂-NPs and a treatment set of colonies was cultured at a concentrations or dose of TiO₂-NPs = 400 ppm. In this study, we have applied a fractal index as key parameter to characterize the colony morphology that features the growth.

Growth and development of living organism populations shows a great variety of geometrical shapes. The aim of the present study was to investigate the effect of TiO₂-NPs on the colony morphology of tumor cell colony in vitro. Our results demonstrate that it is possible to describe how a cell colony adapts itself to external changes, from morphological points of view. However, the way in which an ensemble of cells forms a colony, usually via cell motility and cell-cell adhesion, is not fully understood at the sub-cellular level. More experimental and theoretical works especially with regards to the mechanism aspect are needed.

Fig. 6 shows typical colonies at different culture conditions, namely with control and treatment conditions. It was clearly observed that colony growth is morphologically changed from control when treated with TiO₂-NPs. It was also found that, these colonies were abnormal in shape and size. In addition, the size of the control colonies appeared to be larger than those of treated group as seen in Fig. 7. The mean diameter \pm SEM of the colonies in untreated cultures was $1,161.302 \pm 219.566 \mu\text{m}$, $N = 25$, while that of the cultures treated with TiO₂-NPs was $852.284 \pm 206.497 \mu\text{m}$ (see table 1). Due to the aggregation TiO₂-NPs, the resulting larger sized particles were observable through naked eyes in black dots or patches. This data may evidently indicate the spread and the adsorption of particles which could affect the growth of colonies. However, it should be noted that only the larger sized particles were observed either through naked eyes or OM. The nanosize-particles could be observed by a more powerful microscope such as Scanning Electron Microscope (SEM), Transmission Electron Microscope (TEM), or Atomic Force Microscope (AFM), etc.

In Fig. 8, it was found that the box-counting fractal dimension, Df, of individual colonies was increased substantially over that in control cultures. The mean Df \pm SEM of the colonies in untreated cultures was 1.0852 ± 0.0197 , $N = 25$ and in cultures treated with TiO₂-NPs 1.2870 ± 0.0454 (see Table I). The standard deviation, it reflected that the morphologies of abnormal or treated colonies are more rough and fluctuated compared to those of the control samples, which appeared to be more uniform and consistent in shape. It should be noted that all the data in this study show fractal dimensions whose complexity is between a straight line (Df = 1) and a circle (Df = 2).

In Fig. 9, to correlate the morphological changes in fractal dimensions with other well known geometrical parameters, we

calculated the circularity and diameter length using the same software, imageJ. It was found that the circularity of the control group (0.4015 ± 0.07100) is higher than that of the treated group (0.103 ± 0.0421). The same tendency was found in the diameter parameter which is $1161.302 \pm 219.5663 \mu\text{m}$ and $852.284 \pm 206.4976 \mu\text{m}$ for the control and treated groups, respectively. In other words, the degree of roughness of colony boundary of the treated samples is significantly larger than that of the control group as clearly seen from fractal dimension and circularity parameters. The irregular boundaries of tumors can be examined by fractal geometric analysis. Indeed, the box counting method reveals that morphological patterns of the higher order, such as gland-like structures or populations of differentiating cancer cells, possess fractal dimension and self-similarity. Since fractal space is not filled out randomly, a variety of morphological patterns or a functional state arises.

On comparing our results with other studies of the TiO_2 that effects cancer cells, Cai R and coworkers [39] investigated the anti-tumor activity of photoexcited TiO_2 particles on HeLa cells in vitro. They found that cell cultures were completely killed in the presence of TiO_2 (50 micrograms/ml) with 10-min UV irradiation by a 500-W-Hg lamp. In contrast, very little cell death was observed from TiO_2 treatment without UV irradiation. They also suggested that the cells were killed by the OH^- and H_2O_2 produced from photoexcited TiO_2 particles. Kubota Y and co-workers [40] studied photokilling of TiO_2 on T-24 human bladder cancer. Here, a distinct cell killing effect was observed on cultured T-24 human bladder cancer cells treated with TiO_2 plus UV light. They also discussed the possible application of photoexcited TiO_2 particles to cancer treatment as a new anti-cancer modality. Ai-Ping Zhang and Yan-Ping Sun [5] investigated the photocatalytic killing effect of photoexcited TiO_2 nanoparticles on human colon carcinoma cell line (LS-174-t) and studied the mechanism underlying the action of photoexcited TiO_2 -NPs on malignant cells. When the concentration of TiO_2 was below 200 mg/mL, the photocatalytic killing effect on human colon carcinoma cells was almost the same as that of UVA irradiation alone. When the concentration of TiO_2 was above 200 mg/mL, the remarkable killing effect of photoexcited TiO_2 -NPs could be found. On comparing previous findings with our results, in which samples were treated with TiO_2 -NPs alone in the dark, our findings seem to reveal surprisingly new findings. To our knowledge, these results are the first that show the significant toxicity effects of TiO_2 -NPs on biological systems under dark condition. This may be partly because of the particle size and/or the chosen measurement index.

To relate our fractal results with the previous ones, we refer to the concept and measurement of fractal dimension by the box-counting method given by [36],[37],[38]. Malignant melanomas in vivo have been investigated and it has been found that the fractal dimension of the boundary of the tumor lies mainly in the range 1.05-1.30 [36],[37] while published experimental data for in vitro and in vivo study of the

boundary of human and animal solid tumors giving with Df in the range 1.09-1.34. Our mean fractal dimension of normal tumor colonies lies in the range 1.0454-1.1129, which agrees well with previous reports, while that of the abnormal colonies lies in the range 1.1848-1.3875 which is relatively high. This evidence may benefit, for example, the clinical trials to be used as an alternative indicator for treatment response of cancers. From biophysics view point, one of the possible explanations of the irregular shape of a colony may be as follows. Due the difference in wave propagation velocities of tumor cell wave (especially at the boundary which are mostly proliferating cells), fluctuations in the number of cell at the front or rim would cause irregularities of its shape and produce irregular cell clusters. Thus, the variety of structural metamorphoses in tumor population waves can be explained both by general approach to their description and by considering individual behavior of cell, with only local interactions between them. These phenomena may be dependent on the essential role of density fluctuations and cell motility in the development of fractal structures. In this particular case where the tumor cells are under the applied stress by being exposed to the TiO_2 -NPs, the changes in colony morphology may be due to the effect of TiO_2 -NPs that decelerates the proliferation of tumor cells by changing the cell properties. This results in cell death which leads to the loss of adhesion of cells to their substrate leading to the colony change. Another possible explanation may be that the colony should grow until it reaches optimal size; then, all further net energy intake should be allocated to reproduction. This means that the optimal colony size is substantially smaller than the maximum possible colony size when all incoming energy is allocated to maintenance and none is available for reproduction.

IV. CONCLUDING REMARKS

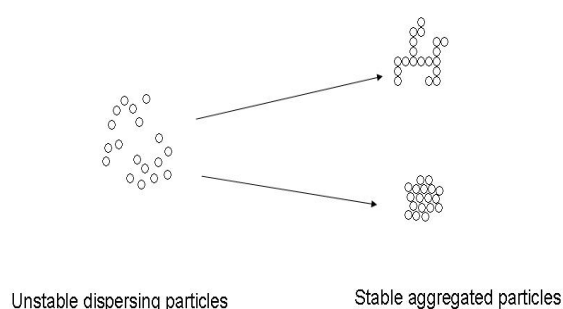
In conclusion, using fractal dimension as a key index for morphological characterization, this paper shows that TiO_2 -NPs modify the dynamics of cell colony growth, causing its eventual arrest and resulting in the colony pattern deformation. These findings are somewhat unexpected because the TiO_2 -NPs treatment was performed in the dark. Hence, no photocatalytic impact via ROS accounts for the changes. This may emphasize the importance of NPs over MPs. Though the use of fractal index does not normally reveal much about the biological mechanism involved, we believe that fractal analysis here shows its promise as an objective measure of seemingly random structures and as a tool for examining the mechanistic origins of pathological forms. Our results indicate that fractal dimension can serve as a useful feature, by itself or in conjunction with other shape features, in the classification of cancer colonies. It should be noted that a general classification of cell colonies or tumors regarding their fractal dimensions could be misleading. However, study of the fractal structure has intensified on a number of biological structures and their growth patterns in past recent

years. Emerging data show that variation in the fractal dimensions may serve as an indicator or predictive factor in normal versus disease conditions, serving as an objective means to guide the clinicians.

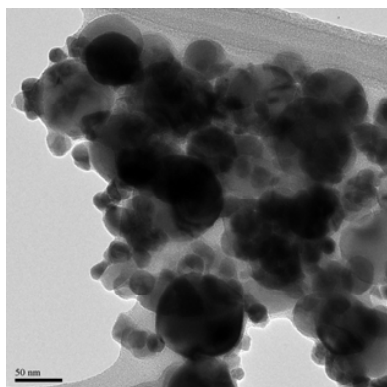
V. ACKNOWLEDGEMENT

We would like to thank our colleagues in Biophysics group at Mahidol University for technical assistance and helpful discussion. This research work was financially supported in part by The Thailand Research Fund (TRF), the National Center for Engineering and Biotechnology, Thailand (BIOTEC), the Institute of Innovation and Development of Learning Process (IIDLP), The Third World Academy of Sciences (TWAS) and Institute of Science and Technology for Research and Development, Mahidol University.

APPENDIX



(a)



(b)

Fig. 1 (a) Schematic picture of unstable dispersing TiO_2 nanoparticles (left) and more stable TiO_2 aggregated particles (right). (b) TEM micrograph of the TiO_2 nanoparticles used in our experiments. The samples were examined under a transmission electron microscope (TECNAI 20) with magnification $\times 29,000$

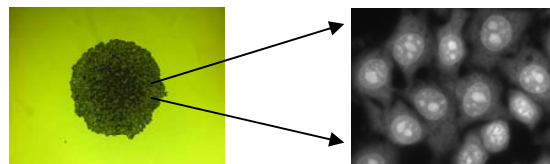


Fig. 2 Example of HeLa cell colony under normal condition (left) and typical individual cells (right). The samples were prepared using the techniques as described in text

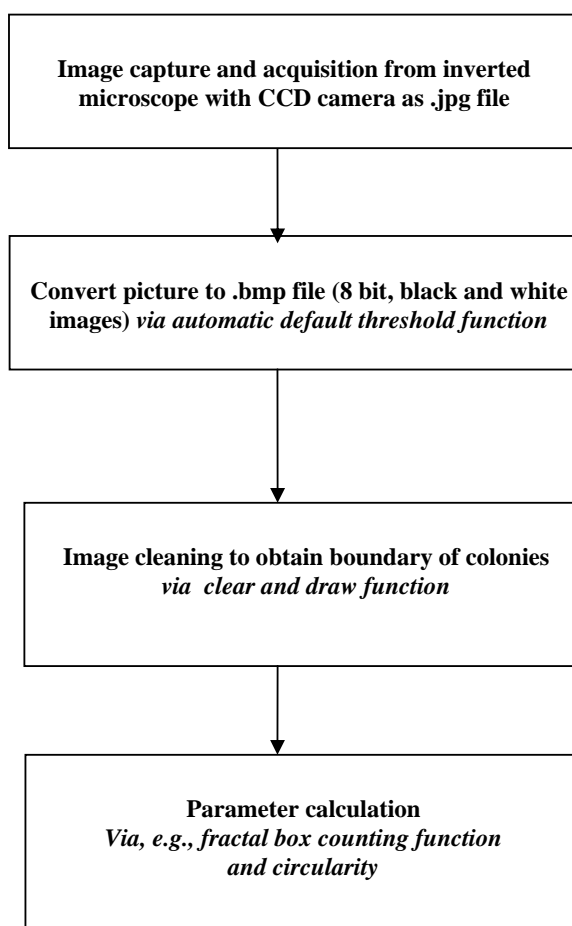


Fig. 3 Flowchart of procedures of image acquisition and parameter calculations

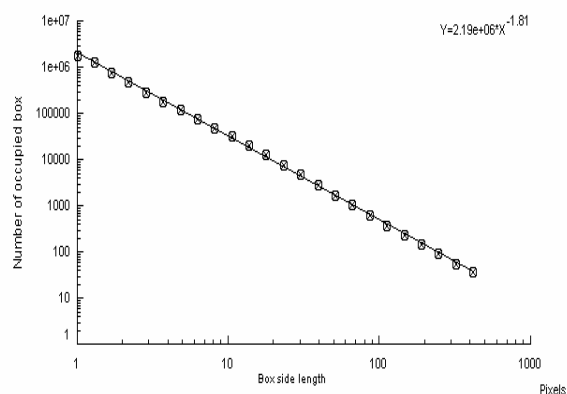
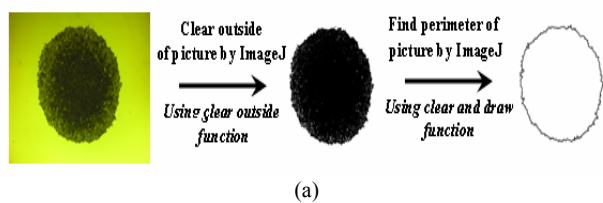


Fig. 4 The fractal dimension interface from imageJ: (a) Diagram of image processing sequence, (b) showing the regression Log-Log plot of boxside-length vs. occupied box number for estimation of fractal dimension

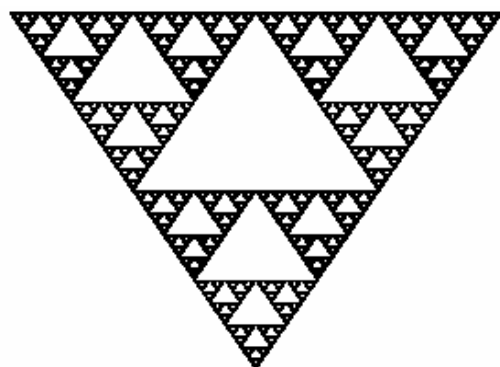
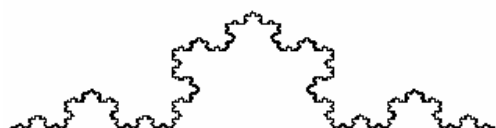


Fig. 5 Tested fractal objects for reliability of the fractal estimation software using in comparison with known theoretical results. Using (a) Koch Curve 6 and (b) Sierpinski Gasket 12. The tests were performed using ImageJ. The test results give: Koch Curve 6 theory =1.262, ImageJ =1.2229, error = 3.098 %, Sierpinski Gasket 12, theory=1.585, ImageJ=1.6015, error = 1.041%.

TABLE I
MEAN VALUES (+/- SEM) OF CELL COLONIES

Parameters	CONTROL GROUP	Treated group
Cell colony Fractal dimension	1.0852±0.019	1.287±0.045
Cell colony circularity	0.4015±0.071	0.103±0.042
Cell colony diameter(μm)	1,161.30±219.56	852.28±206.50

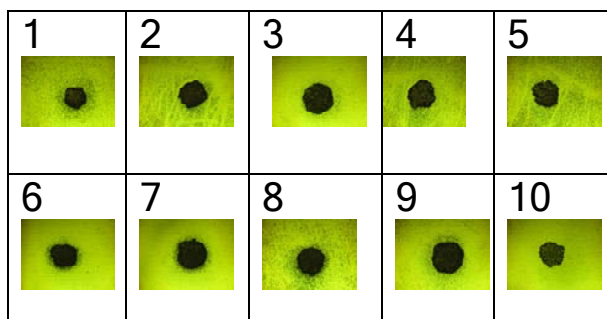
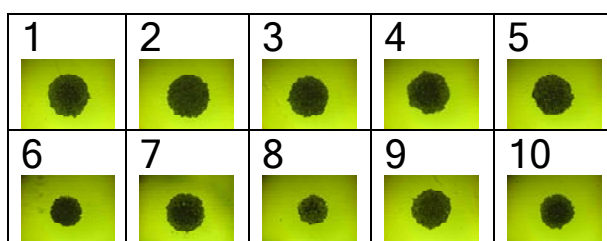


Fig. 6 Experimental data of typical colonies : (a) control or untreated colonies and (b) colonies treated with 400 ppm. of TiO_2 - NPs

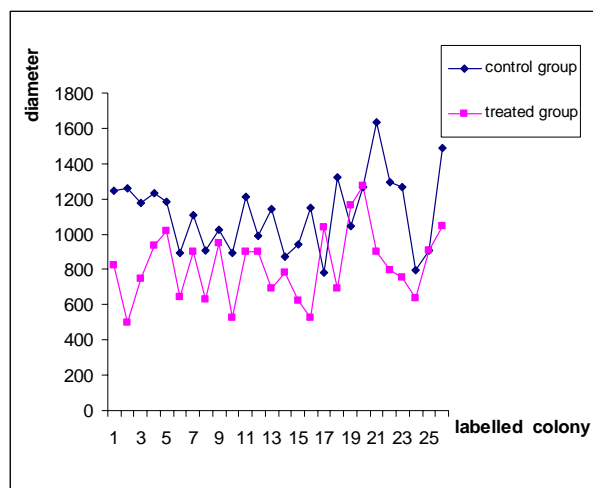


Fig 7 A comparison between the variation in colony diameter length of HeLa cells of the control and 400ppm TiO_2 -NPs treatment. The diameter lengths of the colonies in control group are larger than those treated by TiO_2 -NPs

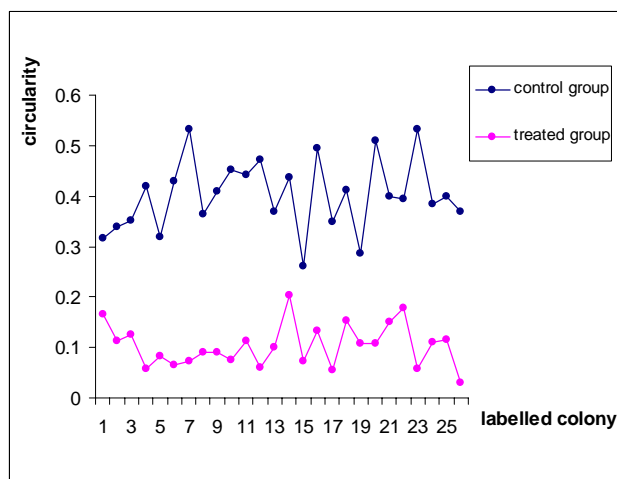


Fig. 9 A comparison between the variation in colony circularity of HeLa cells of the control and 400ppm TiO_2 -NPs treatment. The circularities of the colonies in control group are larger than those treated by TiO_2 -NPs

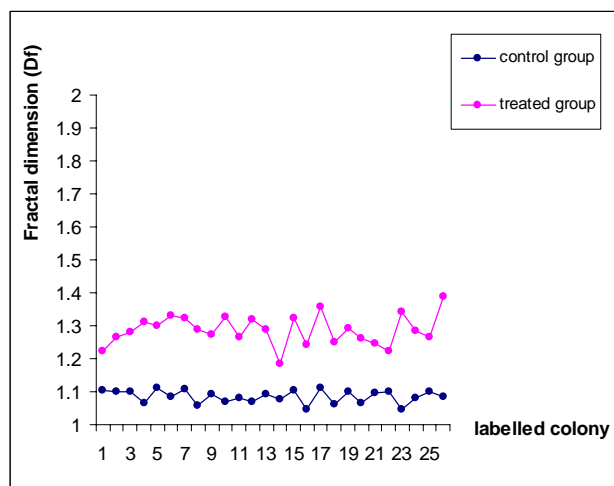


Fig. 8 Fractal dimensions of tumor boundaries at different conditions, namely control and TiO_2 treatment conditions. The data shows that the Df of the treated group (1.2870 ± 0.0454) are systematically larger than those of control group (1.0852 ± 0.0197). It also clearly illustrates that the shape treated samples is more diverse and rough on the surface

REFERENCES

- [1] Alivisatos A. Semiconductor Clusters, Nanocrystals and Quantum Dots Science of The Total Environment 271(5251): 933 – 937, 1996.
- [2] Schwarzer H, Peukert W. Prediction of aggregation kinetics based on surface properties of nanoparticles. Chem Eng Sci 60:11-25, 2005.
- [3] Hunter R. Foundations of colloid Science University Press, Oxford, Great Britain. I, II
- [4] Waliszewski P. Complexity, dynamic cellular network, and tumour-genesis. Pol J Pathol 46:235-41,1997
- [5] Zhang A, Sun Y. Photocatalytic killing effect of TiO_2 nanoparticles on Ls-174-t human colon carcinoma cells. World J Gastroenterol. 10(21):3191-3193,2004
- [6] Hoffmann M, Martin ST, Choi WY, Bahnemann DW. Environmental Applications of Semiconductor Photocatalysis. Chem Rev 95:65.1995
- [7] Maness P, Snolinski S, Blake D, Wolfrum Z, Jacoby W. Solar Treatment as an Alternative for Water Disinfections. Appl Environ Microbiol 65:4094,1999
- [8] Heller A. Preparation of Ti-Si binary oxide thin film photocatalysts by the application of anionized cluster beam method. Acc. Chem. Res 28:503-508,1995
- [9] Ollis D, Pelizzetti E, Serpone N. Environmental Applications of Semiconductor Photocatalysis. Environ. Sci. Technol 25:1523-1529,1991
- [10] Sitkiewitz S, Heller A. Photocatalytic oxidation of benzene and steatic on sol-gel derived TiO_2 thin films attached to glass. New J. Chem 20:233-241,1996
- [11] Uchida H, Itoh S, Yoneyama H. Photocatalytic Decomposition of Propyzamide Using TiO_2 Supported on Activated Carbon. Chem. Lett. 1995-1998, 1993.
- [12] Cai R, Hashimoto K, Itoh K, Kubota Y, Fujishima A. Photokilling of malignant cells with Ultrafine TiO_2 powder. Bull. Chem. Soc. Jpn 64:1268-1273, 1991.
- [13] Ireland J, Klostermann P, Rice E, Clark R. Inactivation of Escherichia coli by titanium dioxide photocatalytic oxidation. Appl. Environ. Microbiol. 59:1668-1670, 1993.
- [14] Matsunaga T, Okochi M. TiO_2 -mediated photochemical disinfection of Escherichia coli using optical fibers. Environ. Sci. Technol 29:501-505, 1995.
- [15] Watts RJ, Kong S, Orr MP, Mille rGC, Henry BE. Photocatalytic Degradation of Toxins Secreted to Water by Cyanobacteria and Unicellular Algae and Photocatalytic Degradation of The Cells of Selected Microorganisms. Water Research 29:95-100. 1995.

- [16] Wei C, Lin W-Y, Zainal Z, Williams N, Zhu K, Kruzic A, Smith R, Rajeshwar K. Bactericidal Activity of TiO₂ Photocatalysts in Aqueous Media: Towards a Solar-Assisted Water Disinfection System". *Environ. Sci. Technol.* 28:934-938, 1994.
- [17] Kikuchi Y, Sunada K, Iyoda T, Hashimoto K, Fujishima A. Photocatalytic bactericidal effect of TiO₂ thin films: dynamic view of the active oxygen species responsible for the effect. *J. Photochem. Photobiol. A: Chem* 106:51-56, 1997.
- [18] Minhua X, Jianamin M, Jianhua G, Zuhong L. Photocatalytic TiO₂ nanoparticles damage to cellular membranes and genetic supramolecules, *Suptamolecular. Science* 5:511-513, 1998.
- [19] Mandelbrot B. How long is the coast of Britain? Statistical self-similarity and fractional dimension. *Science* 156:636-8, 1997.
- [20] BB. M. The fractal geometry of nature. Freeman, San Francisco. 1983.
- [21] Mach J, Mas F, Sagués F. Laplacian multifractality of growth probability distribution in electrodeposition. *Europhys. Lett* 25:271-27, 1994.
- [22] Shlesinger M, West B. Complex fractal dimension of the bronchial tree. *Phys. Rev. Lett* 67:2106-2108, 1991.
- [23] Burlando B. The fractal dimension of taxonomic systems. *J. Theor. Biol* 146:99-114, 1990.
- [24] Goldberger AG, AN-IdfcCt, fractals, and complexity at the bedside. *Lancet* 347:1312-1314. Non-linear dynamics for clinicians: Chaos theory, fractals, and complexity at the bedside. *Lancet* 347:1312-1314, 1996.
- [25] Churilla A, Gottschalke W, Liebovitch Lea. Membrane potential fluctuations of human T-lymphocytes have fractal characteristics of fractional Brownian motion. *Ann Biomed Eng* 24:99-108, 1996.
- [26] Family F, Masters B, Platt D. Fractal pattern formation in human retinal vessels. *Physica D: Nonlinear Phenomena* 38:98, 1989.
- [27] Fujikawa H, Matsushita M. Fractal growth of *Bacillus subtilis* on agar plates. *J. Phys. Soc. Jpn* 58:3875-3878, 1998.
- [28] Gitter J, Czerniecki M. Fractal analysis of the electromyographic interference pattern. *J. Neurosci Methods* 58:103-108, 1995.
- [29] Ito K, Gunji Y. Self-organization of living systems towards criticality at the edge of chaos. *Biosystems* 33:17-24, 1994.
- [30] Macheras P, Argyrakakis P, Polymilis C. Fractal geometry, fractal kinetics and chaos en route to biopharmaceutical sciences. *Eur J Drug Metab Pharmacokinet* 21:77-86, 1996.
- [31] Mainster M. The fractal properties of retinal vessels: Embryological and clinical implications. *Eye* 4:235, 1990.
- [32] Ragazzi E. Hidden fractals in pharmacodynamics. *Pharmazie* 50:66-68 1995.
- [33] Smith TJ, Marks W, Lange Gea. A fractal analysis of cell images. *J Neurosci Methods* 27:173-180, 1998.
- [34] Turcott R, Teich M. Fractal character of the electrocardiogram: Distinguishing heart-failure and normal patients. *Ann Biomed Eng* 24:269-293, 1996.
- [35] Williams N. Fractal geometry gets the measure of life's scales. *Science* 276 :34, 1997.
- [36] Bru A, Albertos S, Subiza J, Garcia-Asenjo JL, Bru I. The Universal Dynamics of Tumor Growth. *Biophysic Journal* 85:2948-2961, 2003.
- [37] Cross S. Fractals in Pathology. *J. Pathol* 182:1-8, 1997.
- [38] Laird A. Dynamics of tumor growth: comparison of Growth rates and extrapolation of growth curve to one cell. *Br J Cancer* 19:278-291, 1964.
- [39] Cai R, Kubota Y, Shuin T, Sakai H, Hashimoto K, Fujishima A. Induction of cytotoxicity by photoexcited TiO₂ particles. *Cancer Res* 52(8): 2346-8., 1992.
- [40] Kubota Y, Shuin T, Kawasaki C, Hosaka M, Kitamura H, Cai R, Sakai H, Hashimoto K, Fujishima A. Photokilling of T-24 human bladder cancer cells with titanium dioxide. *Br. J. Cancer. Dec* 70(6): 1107-11, 1994.